New paradigm for configurational entropy in glass-forming systems

Aleksandra Drozd-Rzoska
Institute of High Pressure Physics
Sylwester J. Rzoska
Institute of High Pressure Physics
Szymon Starzonek (starzoneks@unipress.waw.pl)
Institute of High Pressure Physics

Research Article

Keywords: Kauzmann temperature, local symmetry, distortions-sensitive, solid-state physics, chemical physics

Posted Date: August 26th, 2021

DOI: https://doi.org/10.21203/rs.3.rs-841680/v1

New paradigm for configurational entropy in glass-forming systems

Aleksandra Drozd-Rzoska, Sylwester J. Rzoska, Szymon Starzonek

Institute of High Pressure Physics of the Polish Academy of Sciences, Warsaw, Poland

Abstract

We show that on cooling towards glass transition configurational entropy exhibits more significant changes than predicted by classic relation. A universal formula according to Kauzmann temperature T_K is given: $S = S_0 t^n$, where $t = (T - T_K)/T$. The exponent n is hypothetically linked to dominated local symmetry. Such a behaviour is coupled to previtreous evolution of heat capacity $\Delta C_P^{config.}(T) = (nC/T)(1 - T_K/T)^{n-1}$ associated with finite temperature singularity. These lead to generalised VFT relation, for which the basic equation is retrieved. For many glass-formers, basic VFT equation may have only an effective meaning. A universal-like reliability of the Stickel operator analysis for detecting dynamic crossover phenomenon is also questioned. Notably, distortions-sensitive and derivative-based analysis focused on previtreous changes of configurational entropy and heat capacity for glycerol, ethanol and liquid crystal is applied.

Introduction

Glass transition has remained a grand cognitive challenge of solid-state physics, chemical physics and material engineering for decades.[1,2] The hallmark feature is Super-Arrhenius (SA) previtreous behaviour of such dynamic properties as the primary relaxation time $\tau(T)$ or viscosity $\eta(T)$:[2,3]

$$\tau(T) = \tau_\infty \, exp\left(\frac{E_a(T)}{RT}\right) \qquad \eta(T) = \eta_\infty \, exp\left(\frac{E_a(T)}{RT}\right) \qquad (1)$$

where $T > T_g$, and $E_a(T)$ is the apparent activation energy. Basic Arrhenius behaviour is retrieved for $E_a(T) = E_a = const$ in the given temperature domain. T_g denotes glass temperature, which is empirically linked to $\tau(T_g) = 100$ s, and $\eta(T_g) = 10^{13}$ P.[4,5]

General SA portrayal of previtreous dynamics described by Eq. (1) has a rational meaning and cannot be used to parameterize experimental data, due to unknown form of activation energy $E_a(T)$.[3] Consequently, replacement relations must be applied. The dominant one is the Vogel-Fulcher-Tammann (VFT) dependence:[2,8]

$$\tau(T) = \tau_\infty \, exp\left(\frac{A_{VFT}}{T-T_0}\right) = \tau_\infty \, exp\left(\frac{D_T T_0}{T-T_0}\right) \qquad (2)$$

where $T > T_g$, the amplitude $A_{VFT} = D_T T_0 = const$, D_T is fragility strength coefficient, T_0 denotes extrapolated singular temperature $T_0 < T_g$. The fragility $\left[m = d\, log_{10}\, \tau\,(T)/d\left(T_g/T\right)\right]_{T=T_g}$ is the key metric of the SA dynamics, indicating a deviation from the Arrhenius behaviour related to $m_{min.} = log_{10}\, \tau(T_g) - log_{10}\, \tau_\infty = 2 - log_{10}\, \tau_\infty$. It is often estimated by the use of the fragility strength coefficient, namely: $m = D_T T_0 T_g / \left(T_g - T_0\right)^2 \, ln\, 1\, 0$, and $m = m(1 + ln\, 1\, 0/D_T)_{min}$.[2,4,5] The enormous popularity of the VFT relation, illustrated in Fig. 1, causes that it is often indicated as an empirical 'universal' scaling pattern for previtreous dynamics. Consequently, its derivations are often treated as a checkpoint for glass transition models.[9-14]

The emergence of previtreous dynamics is associated with passing a melting temperature without crystallization and entering a metastable, supercooled domain.[2,13,14] In many 'predominantly' glass-forming systems, being of a particular interest of glass transition physics, supercooling is possible at any practical cooling rate, facilitating broadband dielectric spectroscopy (BDS) studies. In the previtreous domain, BDS requires frequency scans of electric impedance ranging from seconds to hours near T_g. BDS studies deliver high-resolution estimations of primary (α, structural) relaxation time from loss curve peak frequency $\tau = 1/2\pi f_{peak}$. Previtreous changes of $\tau(T)$ are recognised as a basic characterization of previtreous SA dynamics.[2-5,13,14]

Configurational entropy (S_C) is an essential thermodynamic characteristic of previtreous domain.[2-5,10,11,13-24] It describes a non-equilibrium entropy excess, taking entropy of equilibrium crystalline state as a reference. In 1948 Walter Kauzmann indicated that for some extrapolated temperature, hidden in a solid amorphous glass state one should expect $S_C(T \to T_K) \to 0$, usually 20-50 K below T_g.[15] The challenge associated with configurational entropy and the Kauzmann temperature T_K explains the recent resume-report:[22] '*The configurational entropy is one of the most important thermodynamic quantities characterizing supercooled liquids approaching the glass transition. Despite decades of experimental, theoretical, and computational investigation, a widely accepted definition of the configurational entropy is missing, its quantitative characterization remains fraught with difficulties, misconceptions, and paradoxes, …practical measurements necessarily require approximations that make its physical interpretation delicate… the Kauzmann transition remains a valid and useful hypothesis to interpret glass*

formation. We also insisted that this is still a hypothesis but in no way a proven or necessary fact…'.

Following above, for an ultimate cognitive insight into glass transition phenomenon, crucial may be a reliable experimental evidence for $S_C(T)$ behavior, matched to clearly non-biased estimation of T_K, and a non-ambiguous link to dynamics.

Experimentally, the configurational entropy is estimated from an evolution of a heat capacity $\Delta C_P(T)$:[2,14,17,18,22,23]

$$S_C(T) = \int_{T_K}^{T} \frac{\Delta C_P(T)}{T} dT \quad (3)$$

where $\Delta C_P(T) = C_P^{SL} - C_P^{glass} = \Delta C_P^{config.}$, with the heat capacity of glass instead of hardly detectable for 'predominant' glass formers, solid crystal entropy changes.

Assuming:

$$\Delta C_P(T) = \frac{\Delta C_P}{T} \quad (4)$$

with $\Delta C_P = const$, one obtains from Eq. (3) the 'classic', dependence for the configurational entropy:[2,17,18]

$$S_C(T) = S_0\left(1 - \frac{T_K}{T}\right) = S_0\left(\frac{T-T_K}{T}\right) = S_0 t \quad (5)$$

where $t = (T - T_K)/T$.

It is commonly used for describing changes of the configurational entropy in previtreous domain and an estimation of T_K.[2,4,16-24] One of the most inspiring models for glass transition was proposed by Adam and Gibbs (AG), five decades ago.[10] It links previtreous slowing-down to cooperatively rearranged regions (CRR), which influence configurational entropy, leading to following relation for previtreous changes of relaxation time:[10]

$$\tau(T) = \tau_\infty \, exp\left(\frac{A_{AG}}{T S_C(T)}\right) \quad (6)$$

where $A_{AG} = const$ is the AG model amplitude.

Substitution of Eq. (5) into Eq. (6) yields the VFT relation, if $T_0 \approx T_K$.[2,10,14] Numerous reports empirically support such a coincidence between a 'dynamic' and 'thermodynamic' singular temperatures for glass-forming systems.[2,3,9-14,21-23] Such an agreement also constitutes an essential reference for a set of theoretical models which link a finite temperature singularity in dynamics to a 'hidden' phase transition. [2,3,9-14,21-23] These empirical and theoretical correlations between 'thermodynamic' and 'dynamic' characterizations of previtreous domain, matched to enormous popularity of the VFT Eq. (2), significantly support Eq. (5) for describing configurational entropy and its usage as a tool for determining T_K.

However, there are blots and non-coherences on the above landscape. Eq. (5) poorly reproduce a variety of observed patterns for the heat capacity (see conclusions section) for $T \to T_g$ (see Fig. 5). As an empirical solution of this problem a relation $\Delta C_P^{conf.}(T) = \Delta C_P / T^{\vartheta}$, with power exponent $0 < \vartheta < 2$ adjusted to a given glass former, was introduced.[25] However, it does not yield a coherent relation for configurational entropy and its model-basis is not clear. In 2003, Tanaka[26] carried out state-of-the-art validation tests of the VFT equation for 52 glass-forming systems and showed that $0.8 < T_0/T_K < 2.2$, i.e., the correlation $T_0 \approx T_K$ appears only for a limited number of glass formers. There is also growing evidence questioning the omnipotence and a fundamental reliability of the VFT relation. It bases mainly on a comparison between experimental data and their scaling via VFT and other model relations. Subsequently, using visual or analytic-residual assessment of fitting quality, the VFT or other relations' prevalence is tested. However, observed discrepancies are subtle, occur only in some temperature domains and they are close to an experimental error limit.[2,13,14,27-31] Consequently, such tests cannot yield

decisive conclusions. Another type of validation of scaling relations is based on a superposition of $\tau(T)$ or $\eta(T)$ experimental data for a dozen glass-forming systems, using model-related parameters with individually selected (fitted) values for each tested system.[2,13,14,32-35] In the authors' opinion, such a model-dependent scaling approach has tautological features and cannot lead to a breakthrough model-validation.

The recalled above record of puzzling results focused on confirming or rejecting the fundamental validity of the VFT relation had to be carried out for $T > T_g$, i.e., 20-50 K above singular temperatures (T_K, T_0). However, remote from singular temperatures, only subtle discrepancies between experimental data and model relations may be expected. An experimental error notably amplifies such a problem. Relatively strong discrepancies between experimental data and scaling relations can be expected only near hypothetical singular temperatures, i.e., in experimentally non-accessible domain.

To address mentioned inherent features of previtreous domain, an analysis concentrated exclusively on subtle distortions between a hypothetical scaling relation and experimental data may be decisive. In Refs. 36-38 linearised derivative-based analysis focused on a portrayal via VFT,[5-8,31,36] MYEGA,[29,37,38] Avramov-Milchev[38, 40] and critical-like[41-43] scaling relations were developed. For instance, the VFT parameterization may validate a linear domain appearing in a plot based on the following transformation of $\tau(T)$ experimental data:[36]

$$\tau(T) \;\rightarrow\; \left[\frac{d\,ln\,\tau(T)}{d(1/T)}\right]^{-1/2} = (D_T T_0)^{-1/2} - T_0(D_T T_0)^{-1/2} \times \frac{1}{T} = A - B \times \frac{1}{T} \qquad (7)$$

Eq. (7), in the form of the plot $\varphi_T = ln\,\tau\,(T)/d(1/T)$ vs. $1/T$, often named 'Stickel operator' analysis,[44] was used earlier for detecting a dynamic crossover temperature T_B, i.e., the crossover between ergodic and non-ergodic previtreous dynamical domains. The appearance of two lines in such a plot and their intersection related to T_B are indicated as a 'universal' feature of previtreous domain.[44-47] Novikov and Sokolov strengthen this 'universality', suggesting a 'magic' time scale $\tau(T_B) = 10^{-7\pm1}$ s, estimated empirically by the 'Stickel-operator' analysis of 30 glass-formers, including low-molecular-weight liquids, polymers, ionic systems, covalent systems and plastic crystals.[48] However, some criticism regarding this finding appeared, due to glass formers with strongly different $\tau(T_B)$ values.[49] Later, Roland showed a pressure-temperature invariance of $\tau(T_B, P_B)$.[50] It is worth nothing, that the linearised distortions-sensitive analysis showed that for glass-forming liquid crystals, plastic crystals and low-molecular-weight liquids with uniaxial molecules as well as a critical-like description are more reliable than the 'classic' VFT description.[42,43]

Hecksher et al.[51] proposed to analyse previtreous dynamics using activation energy index $I_{DO}(T) = -\,d\,ln\,E_a\,(T)/d\,ln\,T = (dE_a/E_a)/(dT/T)$, i.e., to transform experimental data $\tau(T) \rightarrow I_{DO}(T)$. The required apparent activation energy was calculated using the general SA Eq. (1), $E_a(T) = RT\,ln(\tau(T)/\tau_\infty)$, assuming a 'universal' value for pre-factor $\tau_\infty = 10^{-14}$ s. In Ref. 51 the analysis for 42 low-molecular-weight glass formers led to the conclusion: '*…there is no compelling evidence for the Vogel–Fulcher–Tammann (VFT) prediction that the relaxation time diverges at a finite temperature. We conclude that theories with a dynamic divergence of the VFT form lack a direct experimental basis*.' However, results from Ref. 51 might be biased by assuming a 'universal' value for the pre-factor, whereas experimental evidence suggests $10^{-16}s < \tau_\infty < 10^{-10}s$.[36,40] In Ref. 52, apparent activation energy was determined using a protocol avoiding this problem. It is based on a numerical solution of a differential equation directly resulted from the SA Eq. (1) and applied for a given set of $\tau(T)$ experimental data:[52]

$$R\,\frac{d\,ln\,\tau(T)}{d(1/T)} = \frac{1}{T}\frac{dE_a(T)}{d(1/T)} + E_a(T) \qquad (8)$$

The analysis of 26 glass-formers, including low-molecular-weight liquids, polymers, liquid crystals, colloids and even plastic crystals, revealed a common empirical pattern:[52]

$$\frac{1}{I_{DO}(T)} = a + bT \quad (9)$$

This result led to a general 'empirical' relation for the index:[45,46] $1/I_{DO}(T) = nT_0/(T - T_0)$, where T_0 is singular temperature determined from the condition $1/I_{DO}(T_0) = 0$ and the parameter $n = -1/a$. It was found that for tested systems $0.18 < n < 1.6$, and limits were related to domination of translational and orientational symmetries, respectively.[52-54] The previtreous dynamics described by the VFT relation is linked to $n = 1$. Following results mentioned a new relation for the configurational entropy was derived:[52]

$$S_C = S_0\left(1 - \frac{T_K}{T}\right)^n = S_0 t^n \quad (10)$$

The 'classic' Eq. (5) is retrieved for $n = 1$.

Problems of the VFT relation inspired the development of new scaling dependences for the previtreous dynamics. The leading position has gained Mauro-Yue-Ellison-Gupta-Allan (MYEGA) relation, which avoids the finite temperature singularity:[29,37]

$$\tau(T) = \tau_0\, exp\left(\frac{C}{T} exp\left(\frac{K}{T}\right)\right) \quad (11)$$

Notably, it can be approximated by the VFT relation at 'high-temperature' domain:[55]

$$ln(\tau(T)/\tau_0)_{=0} = \frac{C}{T} exp\left(\frac{K}{T}\right) = \frac{C}{T\, exp(-K/T)} \approx \frac{C}{T(1-K/T)} = \frac{C}{T-K} \quad (12)$$

where $K \approx T_0$, and $C \approx D_T T_0$, if comparing with VFT Eq. (2).

Results and Discussion

Figure 1 shows that applications of VFT relation for glass-forming systems permanently increases, despite recalled numerous of objections. One can add to the presented statistics reports using the Williams-Landel-Ferry (WLF) relation,[56] isomorphic to the VFT Eq. (2) and primarily used in polymer physics: 55-70 reports in the last two decades, annually.[57] For comparison, studies exploring MYEGA relation (since 2009) for portraying previtreous dynamics are also shown in Figure 1.

When discussing previtreous behaviour, one may consider substitution of Eq. (10) to the AG model relation Eq. (6). This yields a 'generalised' VFT relation:

$$\tau(T) = \tau_\infty\, exp\left(\frac{S_o A_{AG} T^{n-1}}{(T-T_0)^n}\right) = \tau_\infty\, exp\left(\frac{A_{VFT} T^{n-1}}{(T-T_0)^n}\right) = \tau_\infty\, exp\left[\frac{D_T T_0/T}{t^n}\right] \quad (13)$$

where $t = (T - T_0)/T$. The 'classic' VFT formula (Eq. (2)) is retrieved for $n = 1$.

Eq. (13) has already been used for describing dynamics in glass-forming polyvinylidene difluoride (PVDF), PVDF + Barium-Strontium-Titanate (BST) microparticles composite,[58] and in its parallel form for describing relaxation time in relaxor ceramics.[59] Nevertheless, these tests cannot be considered as a crucial validation of Eq. (13) if recalling the above discussion. The milestone meaning could have derivative-based and distortions-sensitive tests focused directly on $S_C(T)$ experimental data. To fill such a cognitive gap a new solution is proposed in given report.

The analysis presented below explores state-of-the-art experimental results for the configurational entropy for 8 glass-forming liquids: glycerol, ethanol, sorbitol, diethyl phthalate, cycloheptanol, cyclooctanol as well as liquid crystals (5*CB, 8*OCB).[16,19,23] Basing on Eq. (10) one can propose the following distortions-sensitive transformation of experimental data:

$$S_C(T) \rightarrow ln\, S_C(T) = ln\, S_0 + n\, ln(1 - T_K/T) \rightarrow$$
$$d\, ln\, S_C(T)/d(1/T) = nT_K/(1 - T_K/T) \quad (14)$$

Consequently:

$$[d\ ln\ S_C\ (T)/d(1/T)]^{-1} = 1/nT_K - 1/nT = A + B(1/T) \quad (15)$$

Temperature dependence of the configurational entropy $S_C(T)$ of experimental data expressed by Eq. (15) should follow a linear behaviour, yielding optimal values for the reference Eq. (10): $n = 1/B$ and $T_K = B/A$.

Figure 2 presents the configurational entropy evolution for supercooled glycerol, ethanol, sorbitol, cycloheptanol, cyclooctanol, diethyl phthalate, 5*CB and 8*OCB. Curves in the part A of Fig.2 portraying experimental data, for selecting liquids, are related to the 'classic' Eq. (5) (in red) and the 'generalised' Eq. (10) (in blue). The Fig. 2A insert shows experimental data presentation based on a hardly explored scale S_C vs. $1/T$, directly resulted from the Eq. (5). Figure 2B portrays configurational entropy normalised to the Kauzmann temperature T_K calculated from Eq. (10). The insert presents a behaviour of the Eq. (10) with different parameter n, i.e. $0.1 < n < 2$.

Figure 3 presents results of the distortions-sensitive analysis of $S_C(T)$ experimental data based on Eq. (15). The linear behavior suggested by Eq. (15) appears, but with different slopes ($B \sim 1/n$). Obtained parameters for studied glass-forming liquids are collected in Table I. These values are, within the limits of the experimental errors, the same as in Ref. 44, e.g. $n = 1.04$ for glycerol and $n = 1.28$ for ethanol, which were obtained from the analysis of 'dynamic' experimental data $\tau(T) \rightarrow I_{DO}(T)$.

These results indicate that for glycerol and diethyl phthalate one can assume $n = 1$, what leads to the VFT relation for relaxation time and the 'classic' expression for configurational entropy (Eq. (5)). On the other hand, for ethanol, sorbitol, 5*CB and 8*OCB the parameter $n > 1$, what in Ref. 44 was linked to glass former consisted of molecules with the uniaxial symmetry. One can expect that in such a case, the generalised VFT Eq. (13) may offer much more.

The main part of Figure 4 presents previtreous behaviour of primary relaxation time in glycerol and ethanol using Angell plot.[4,5] Fig. 5 shows the linearised distortions-distortions sensitive analysis of data from the central part of the plot, based on Eq. (7). Linear domains indicate the preference for describing $\tau(T)$ changes by the VFT relation (Eq. (2)). Such a behaviour is evidenced for glycerol but absent for ethanol.

Results related to Fig. 4 and Fig. 5 may be considered as the argument against the 'universal' validity of the 'Stickel operator' analysis used for testing dynamic crossover phenomenon,[44-50] due to inherently coupling to pre-assumption of an omnipotent validity of the basic VFT relation. The question also raised for general validity of discussions of fragility, i.e., the key metric for the SA dynamics of the previtreous domain,[2,4,5] within the context of recalled Eq. (2).[2,5,14,57,62-65]

Conclusions

Concluding, the report presents the evidence supporting the 'generalised' relation for the configurational entropy (Eq. (10)) and the protocol for linearised, distortions-sensitive analysis of related experimental data (Eq. (15)). All these lead to corrected values of the Kauzmann temperature. The 'generalised' relation for configurational entropy (Eq. (10)) also leads to the 'generalised' VFT Eq. (13). Its validity indicates the accidental significance of testing the dynamic crossover phenomenon via the 'Stickel operator'[44-50] and problems of discussions focused on fragility within frames of the VFT relation[2,5,14,24,57,62-65]. Some discrepancies between the direct estimation of fragility and fragility strength by the use of VFT equation were raised recently.[64]

The characteristic feature of 'generalised' VFT Eq. (13) is power exponent *n*, influencing a distance from singular temperature distance T_0. Notably, a similar correction was advised in 1984 by Bengtzelius, Götze and Sjölander (BGS)[65], basing on the mode-coupling theory, in 1988 by Bendler and Shlezinger (BS)[66], using the mobile defects ('random walk') approach, as well as Hall and Wolyness[67] for randomly packed spheres (HW):

$$\tau = \tau_\infty \, exp\left(\frac{F}{(T-T_K)^\alpha}\right) \qquad (16)$$

where $\alpha \approx 1.76$ for BGS, $\alpha = 3/2$ for BS, and $\alpha = 2$ for HW models.

More recently, the random first-order transition (RFOT) model resulted in a similar dependence with an exponent $\alpha = \psi/(d-\theta)$,[2] where the exponent *d* is the spatial dimension, θ is for free energy surface cost on linear size of interface between two amorphous states and the exponent ψ is a free energy barrier that must be overcome to rearrange a correlated volume. It is worth stressing that exponent α value, for mentioned models, is located within frames empirically indicated for the exponent *n*.[52]

Returning to the generalised Eq. (10) for configurational entropy, one can derive the relation for previtreous changes of the heat capacity, namely:

$$\Delta C_P^{config.}(T) = T\frac{dS_C}{dT} = \frac{nS_0T_K}{T}\left(1-\frac{T_K}{T}\right)^{n-1} \qquad (17)$$

Heat capacity changes resulted from Eq. (17) are presented in Fig. 6, for the selected terminal, values of parameter *n*. Except the 'classic' case $n = 1$, they show previtreous changes linked to a finite temperature singularity at T_K, which has been not expected for heat capacity so far. The insert in Figure 5 recalls different heat capacity change patterns in a normalised scale for $T \to T_g$. To follow this issue, see also Refs. 68, 69.

One of glass transition experimental features is approaching the hypothetical Kauzmann temperature closer in heat capacity studies by increasing a cooling rate than in BDS tests for which the cooling rate factor is not important. Shifting below the standard T_g value in DTA (differential thermal analysis) studies is often too strong 'anomalous' heat capacity changes. Such a behaviour via singularities appearing in Eq. (17). The description introduced by Eqs. (10) and (17) also correlates with recent indications for more pronounced changes of the configurational entropy than predicted by the classic Eq. (4) or indication for decoupling between VFT based estimations of the fragility (see comments below Eq. (2) and the real value of the fragility determined from the Angell plot (Fig. 4).[63,64]

Notably, hypothetical validity of Eq. (17) opens a new possibility for distortions-sensitive tests directly exploring previtreous changes of the heat capacity:

$$\frac{d\,ln\left(T\Delta C_P^{config.}\right)}{d(1/T)} = \frac{T_K(n-1)}{1-T_K/T} \Rightarrow \left(\frac{d\,ln\left(T\Delta C_P^{config.}\right)}{d(1/T)}\right)^{-1} = T_K(n-1) - \frac{T_K^2(n-1)}{T} = A - \frac{B}{T} \qquad (18)$$

The linear regression fit for a plot based on Eq. (18) may yield A and B coefficients, what gives consequently $T_K = B/A$, $n = A^2/B + 1$.
The glass transition is most often indicated as the dominantly dynamic phenomenon, which heuristically supports impressive previtreous primary relaxation time or viscosity changes. This is supported by dependence of glass temperature and heat capacity behaviour from a cooling. This report proposed that the long-range, previtreous behaviour also occurs for such a basic thermodynamic property as configurational entropy and heat capacity. This may suggest not only dynamic but also thermodynamic character of glass transition.

Acknowledgments

Funding: Studies were carried out due to the National Centre for Science (NCN grants, Poland), ref. 2017/25/B/ST3/02458, headed by Sylwester J. Rzoska, ref. 2016/21/B/ST3/02203, headed by Aleksandra Drozd-Rzoska and 2019/32/T/ST3/00621 headed by Szymon Starzonek.

Author contributions:

Conceptualization: ADR, SJR

Visualization: SJR, SS

Writing – original draft: ADR, SJR

Writing – review & editing: SJR, SS

Competing interests: Authors declare that they have no competing interests.
Data and materials availability: All data are available after personal request.

References

1. D. Kennedy, C. Norman, What don't we know. *Science* **309**, 75 (2005): Special issue for 125 anniversary.
2. P. G. Wolyness and V. Lubchenko, *Structural Glasses and Supercooled Liquids: Theory, Experiment, and Applications* (Wiley & Sons Inc., Hoboken, 2012).
3. L. Berthier, and M. Ediger, Facets of glass physics. *Physics Today* **69**, 41 (2016).
4. C. A. Angell, Formation of glasses from liquids and biopolymers, *Science* **267**, 1924 (1995).
5. R. Böhmer, K. L. Ngai, C. A. Angell, D. J. Plazek, Nonexponential relaxations in strong and fragile glass formers. *J. Chem. Phys*. **99**, 4201 (1993).
6. H. Vogel, Das temperature-abhängigketsgesetz der viskosität von flüssigkeiten. *Phys. Z*. **22**, 645-646 (1921).
7. G. S. Fulcher, Analysis of recent measurements of the viscosity of glasses. *J. Am. Ceram Soc*. **8**, 339–355 (1925).
8. G. Tammann, W. Hesse, Die abhängigkeit der viskosität von der temperatur bei unterkühlten flüssigkeiten. *Z. Anorg. Allg. Chem*. **156**, 245–257 (1926).
9. D. Turnbull, and M. H. Cohen, Free-volume model of the amorphous phase: glass transition. *J. Chem. Phys.* **34**, 120–125 (1961).
10. G. Adam, and J. H. Gibbs, On the temperature dependence of cooperative relaxation properties in glass-forming liquids. *J. Chem. Phys*. **43**, 139 (1965).
11. L. Berthier, G. Biroli, Theoretical perspective on the glass transition and amorphous materials. *Rev. Mod. Phys*. **83**, 587 (2010).
12. H. Tanaka, Critical-like behavior of glass forming liquids. *Nat. Mat*. **9**, 324 (2010).
13. F. Kremer and A. Loidl, *The Scaling of Relaxation Processes* (Springer, Berlin, 2018).
14. R. Ramirez, *An Introduction to Glass Transition* (Nova Sci. Pub., London, 2019).
15. W. Kauzmann, The nature of the glassy state and the behavior of liquids at low temperatures. *Chem. Rev*. **43**, 219 (1948).
16. O. Haida, H. Suga, and S. Seki, Calorimetric study of the glassy state XII. Plural glass-transition phenomena of ethanol. *J. Chem*. *Thermodyn*. **9**, 1133–1148 (1977).
17. C. A. Angel1, Thermodynamic aspects of the glass transition in liquids and plastic crystals. *Pure & Appl*. *Chem*. **63**, 1387-1392 (1991).
18. C. A. Angell, Entropy and fragility in supercooling liquids. *J. Res. Natl. Inst. Stand. & Technol*. **102**, 171-185 (1997).
19. M. A. Ramos, I. M. Shmytko, E. A. Arnautova, R. J. Jimenez-Rioboo. V. Rodriguez-Mora, S. Vieira, M. J. Capitan, On the phase diagram of polymorphic ethanol: Thermodynamic and structural studie.*, J. Non-Cryst. Solids* **352**, 4769–4775 (2006).
20. R. Busch, J. Schrörs, and W. H. Wang, Thermodynamics and kinetics of bulk metallic glass. *MRS Bull*. **32**, 620-623 (2007).
21. O. S. Bakai, On the heterophase liquid thermodynamics and cooperative dynamics, *Condens. Matt. Phys*. **13**, 23604 (2010).
22. L. Berthier, M. Ozawa, C. Scaillet, Configurational entropy of glass-forming liquids. *J. Chem. Phys.* **150**, 160902 (2019).
23. M. Ozawa, C. Scalliet, A. Ninarello, L. Berthier, Does the Adam-Gibbs relation hold in simulated supercooled liquids? *J. Chem. Phys*. **151**, 084504 (2019).

24. Q. Gao and Z. Jian, Predicting the thermodynamic ideal glass transition temperature in glass-forming liquids. *Materials* **13**, 2151 (2020).
25. L.-M. Wang, C. A. Angell, and R. Richert, Fragility and thermodynamics in nonpolymeric glass-forming liquids. *J. Chem. Phys.* **125**, 074505 (2006).
26. H. Tanaka, Relation between thermodynamics and kinetics of glass-forming liquids. *Phys. Rev. Lett.* **90**, 05570 (2003).
27. R. Richert, Scaling vs. Vogel-Fulcher-type structural relaxation in deeply supercooled materials. *Physica A* **287**, 26 (2000).
28. G. B. McKenna, Diverging views on glass transition. *Nat. Phys*. **4**, 673-674 (2008).
29. J. C. Mauro, Y. Yue, A. J. Ellison, P. K. Gupta, and D. C. Allan, Viscosity of glass-forming liquids. *Proc. Natl. Acad. Sci*. *(USA)* **106**, 19780-19784 (2009).
30. P. Lunkenheimer, S. Kastner, M. Köhler, and A. Loidl, Temperature development of glassy α-relaxation dynamics determined by broadband dielectric spectroscopy. *Phys. Rev. E* **81**, 051504 (2010).
31. A. Drozd-Rzoska, S. J. Rzoska, Consistency of the Vogel-Fulcher-Tammann (VFT) equations for the temperature-, pressure-, volume- and density- related evolutions of dynamic properties in supercooled and superpressed glass forming liquids/systems, in S. J. Rzoska, V. Mazur and A. Drozd-Rzoska (eds.), in *Metastable Systems under Pressure*. pp. 93-106 (Springer, Berlin, 2010).
32. E. Rössler, K.-U. Hesse, and V. N. Novikov, Universal representation of viscosity in glass forming liquids. *J. Non-Cryst. Solids* **223**, 207–222 (1998).
33. M. L. Ferreira Nascimento, C. Aparicio, Data classification with the Vogel–Fulcher–Tammann–Hesse viscosity equation using correspondence analysis, *Physica B* **398**, 71-77 (2007).
34. Y. S. Elmatad, R. L. Jack, D. Chandler, and J. P. Garrahan, Finite-temperature critical point of a glass transition. *Proc. Natl. Acad. Sci. USA* **107**, 112793 (2010).
35. J.-H. Hung, T. K. Patra, D. S. Simmons, Forecasting the experimental glass transition from short time relaxation data. J. Non-Cryst.-Solids **544**, 120205 (2020).
36. A. Drozd-Rzoska and S. J. Rzoska, On the derivative-based analysis for temperature and pressure evolution of dielectric relaxation times in vitrifying liquids. *Phys. Rev. E* **73**, 041502 (2006).
37. Q. Zheng, J. C. Mauro, Viscosity of glass-forming liquids. *J. Am. Ceram. Soc*. **100**, 6-25 (2016).
38. J. C. Martinez Garcia, J. Ll. Tamarit and S. J. Rzoska, Enthalpy space analysis of the evolution of the primary relaxation time in ultraslowing systems. *J. Chem. Phys*. **134**, 024512 (2011).
39. I. Avramov, and A. Milchev, Effect of disorder on diffusion and viscosity in condensed systems. *J. Non-Cryst. Solids* **104**, 253 (1988).
40. Drozd-Rzoska, S. J. Rzoska and C. M. Roland, On the pressure evolution of dynamic properties in supercooled liquids. *J. Phys.: Condens. Matt*. **20**, 244103 (2008).
41. Drozd-Rzoska, S. J. Rzoska, M. Paluch, Universal, critical-like scaling of dynamic properties in symmetry-selected glass formers. *J. Chem. Phys.* **129**, 184509 (2009).

42. Drozd-Rzoska, S. J. Rzoska, S. Pawlus, J. C. Martinez-Garcia, and J.-L. Tamarit, Evidence for critical-like behavior in ultraslowing glass-forming systems. *Phys. Rev. E* **82**, 031501 (2010).
43. Drozd-Rzoska, Universal behavior of the apparent fragility in ultraslow glass forming systems. *Sci. Rep*. **9**, 6816 (2019).
44. F. Stickel, E. W. Fisher, and R. Richert, Dynamics of glass-forming liquids. I. Temperature-derivative analysis of dielectric relaxation data. *J. Chem. Phys*. **102**, 6251-6257 (1995).
45. E. Kamińska, K. Kamiński, and M. Paluch, Primary and secondary relaxations in supercooled eugenol and isoeugenol at ambient and elevated pressures: Dependence on chemical microstructure. *J. Chem. Phys.* **124**, 164511 (2006).
46. F. Mallamace, C. Corsaro, H. E. Stanley, S-H. Chen, The role of the dynamic crossover temperature and the arrest in glass-forming fluids, *Europ. Phys. J*. **34**, 94-99 (2011).
47. M. I. Ojovan, On viscous flow in glass-forming organic liquids. *Molecules* **25**, 4029 (2020).
48. V. N. Novikov, and A. P. Sokolov, Universality of the dynamic crossover in glass-forming liquids: a "magic" relaxation time. *Phys. Rev. E* **67**, 031507 (2003).
49. K.L. Ngai, *Relaxation and Diffusion in Complex Systems* (Springer, Berlin, 2011).
50. R. Casalini, M. Paluch, C. M. Roland, Dynamic crossover in Supercooled liquids induced by high pressure. *J. Chem. Phys*. **118**, 5701-5703 (2003).
51. T. Hecksher, A. I. Nielsen, N. B. Olsen, and J. C. Dyre, Little evidence for dynamic divergences in ultraviscous molecular liquids. *Nat. Phys*. **4**, 737–744 (2008).
52. J. C. Martinez-Garcia, S. J. Rzoska, A. Drozd-Rzoska, and J. Martinez-Garcia, A universal description of ultraslow glass dynamics. *Nat. Comm*. **4**, 1823 (2013).
53. J.C. Martinez-Garcia, S. J. Rzoska, A. Drozd-Rzoska, J. Martinez-Garcia, and J. C. Mauro. Divergent dynamics and the Kauzmann temperature in glass forming systems. *Sci. Rep*. **4**, 5160 (2014).
54. J.C. Martinez-Garcia, S. J. Rzoska,, A. Drozd-Rzoska, S. Starzonek, and J. C. Mauro, Fragility and basic process energies in vitrifying systems. *Sci. Rep*. **5**, 8314 (2015).
55. M. Smedskjaer, J. C. Mauro, Y. Z. Yue, Ionic diffusion and the topological origin of fragility in silicate glasses, *J. Chem. Phys*. **131**, 244514 (2009).
56. J. Williams, R. F. Landel, and J. D. Ferry, The temperature dependence of relaxation mechanisms in amorphous polymers and other glass-forming liquids. *J. Am. Chem. Soc*. **77**, 3701-3706 (1955).
57. Y. Shangguan, F. Chen, E. Jia, Y. Lin, J. Hu and Q. Zheng, New insight into time-temperature correlation for polymer relaxations ranging from secondary relaxation to terminal flow: application of a universal and developed WLF equation. *Polymer* **9**, 567 (2017).
58. S. Starzonek, K. Zhang, A. Drozd-Rzoska, S. J. Rzoska, E. Pawlikowska, M. Szafran, and F. Gao, Polyvinylidene difluoride-based composite: glassy dynamics and pretransitional behaviour. *Europ. Phys. J. B*, **93**, 1-10 (2020).
59. R. Levit, J. C. Martinez-Garcia, D. A. Ochoa, J. E. Garcia, The generalized Vogel-Fulcher-Tammann equation for describing the dynamics of relaxor ferroelectrics. *Sci*. *Rep*. **9**, 12390 (2019).
60. S. Pawlus, J. Bartoš, O. Šauša and J. Krištiak, M. Paluch, Positronium annihilation lifetimes and dielectric spectroscopy studies on diethyl phthalate: Phenomenological correlations and

microscopic analyses in terms of the extended free volume model by Cohen-Grest. *J. Chem. Phys*. **124**, 104505 (2006).
61. I. S. Garcia-Colin, L. F. del Castillo, and P. Goldstein, Theoretical basis for the Vogel-Fulcher-Tammann equation. *Phys. Rev. B* **40**, 7040-7044 (1990).
62. Q. Gao and Z. Jian, Predicting the thermodynamic ideal glass transition temperature in glass-forming liquids. *Materials* **13**, 2151 (2020).
63. Q. Gao, Z. Jian, Fragility and Vogel-Fulcher-Tammann parameters near glass transition temperature. *Mat. Chem. and Phys*. **252**, 123252 (2020).
64. C.-S. Lee, M. Lulli, L.-H. Zhang, H.-Y. Deng, and C.-H. Lam, Fragile glasses associated with a dramatic drop of entropy under supercooling. *Phys. Rev. Lett*. **125**, 265703 (2020).
A. Angell, Insights into glass formation and glass transition in supercooled liquids, by study of related phenomena in crystals. *J. Non-Cryst. Solids* **354**, 42-44 (2007).
65. H. Bo Ke, P. Wen, W. H. Wang, The inquiry of liquids and glass transition by heat capacity. *AIP Advances* **2**, 041404 (2012).
66. U. *Bengtzelius,* W. *Götze,* and A. J. *Sjölander,* Dynamics of supercooled liquids and the glass transition. *J. Phys. C*. **17**, 5915 (*1984*).
67. J. Bendler, M. F. Shlezinger, Generalized Vogel law for glass-forming liquids. *J. Stat. Phys*. **53**, 531–541 (1988).
68. R. W. Hall, P. G. Wolyness, The aperiodic crystal picture and free energy barriers in glasses. *J. Chem. Phys*. **86**, 2943-2948 (1987).

Table I Parameters calculated from the distortions-sensitive analysis.

The T_K was calculated directly from the Eq. (10), when the condition $S_C(T) \to 0 \Rightarrow T|_{S_C(T)=0} = T_K$ is fulfilled.

Liquids	Abr.	$T_g^{\spadesuit}$ (K)	$n = 1$		$n \neq 1$		
			T_K (K)	$\Delta T = T_g - T_K$ (K)	n	T_K (K)	$\Delta T = T_g - T_K$ (K)
ethanol	Eth	93.6	77	16.6	1.28	68	25.6
glycerol	Gly	183.5	152	31.5	1.04	149	34.1
sorbitol	Srb	268.1	174	94.1	1.57	140	128.1
cycloheptanol	C7-OH	130.1	48.5	81.6	0.16	116	14.1
cyclooctanol	C8-OH	151.2	61	90.2	0.78	70	81.2
diethyl phtalate	Dep	179.3	38	141.3	0.98	39	140.3
isopentylcyanobiphenyl	5*CB	214.2	165	49.2	1.12	159	55.2
isooctylcyanobiphenyl	8*OCB	221.2	203	18.2	1.51	185	36.2

$^{\spadesuit}$glass temperature calculated for the relaxation time $\tau = 100$ s.

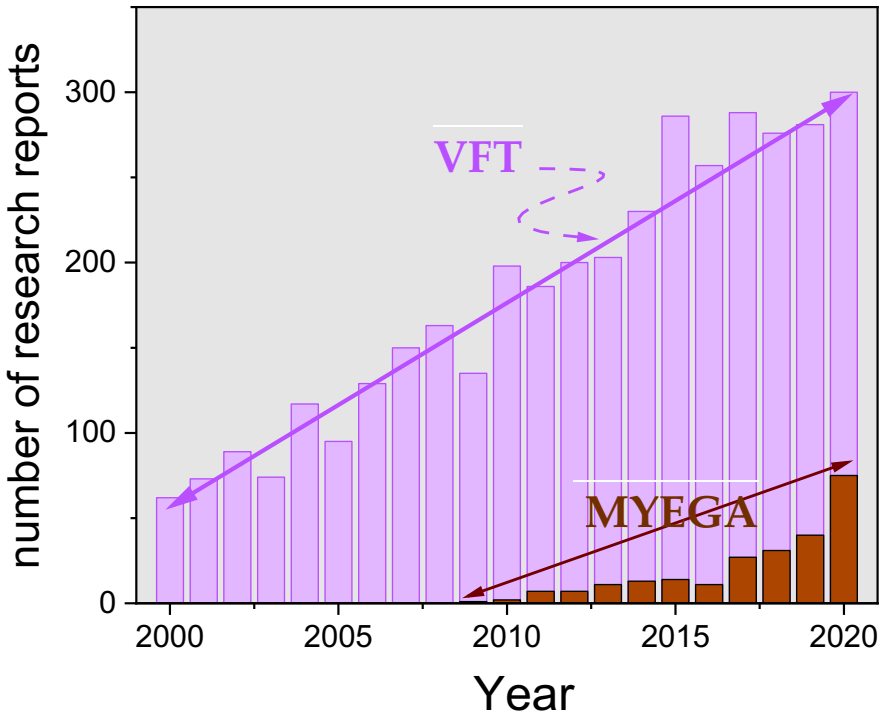

Fig. 1

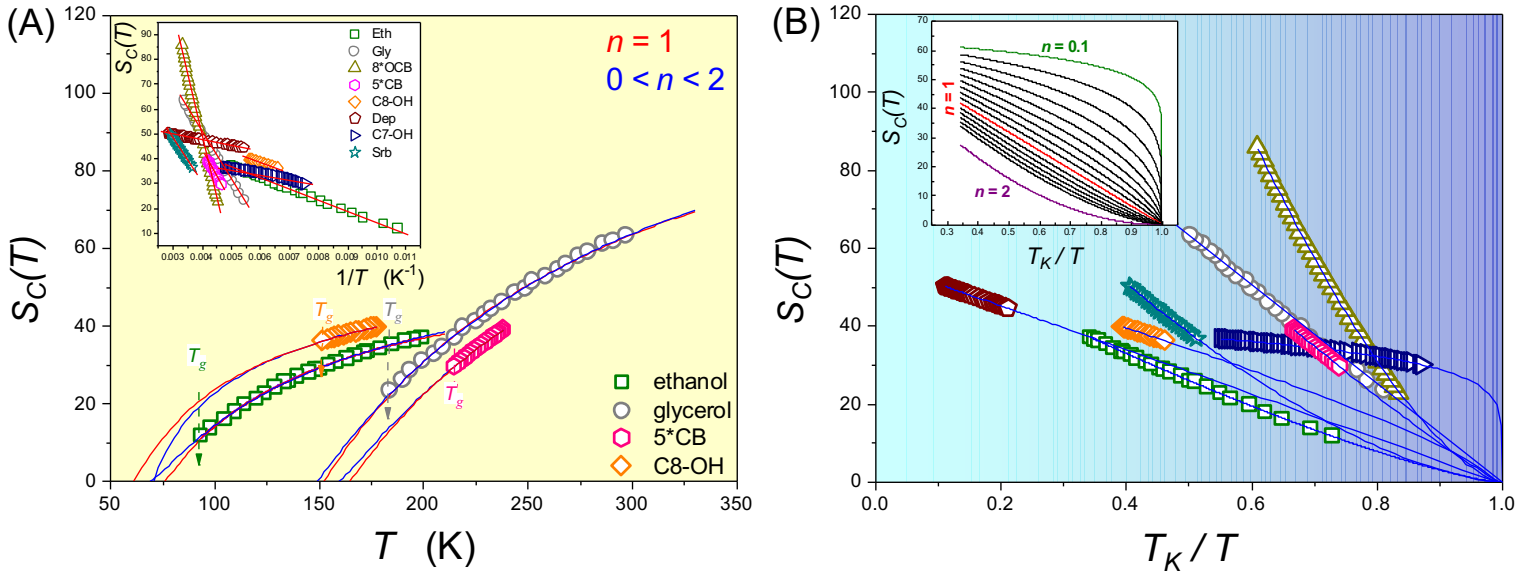

449
450 **Fig. 2**
451

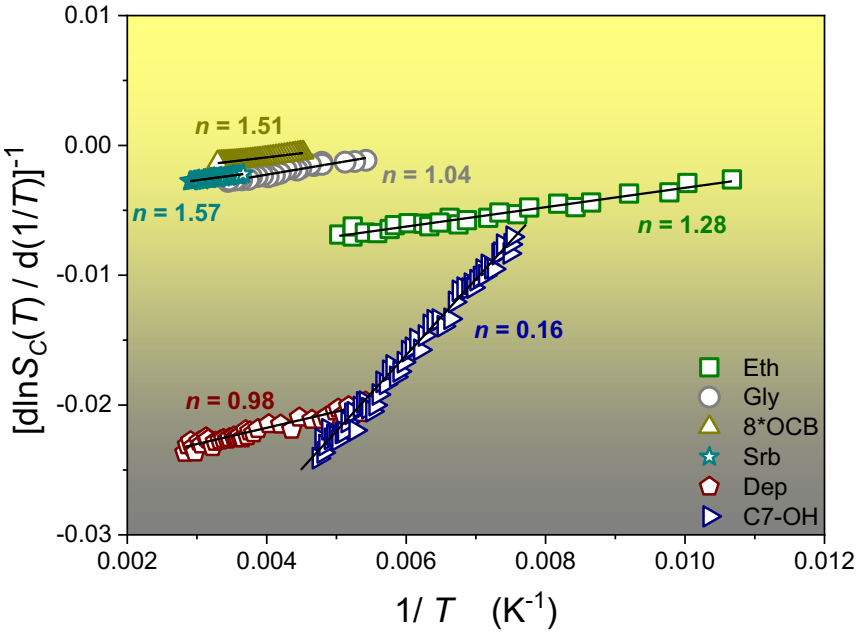

452
453 **Fig. 3**

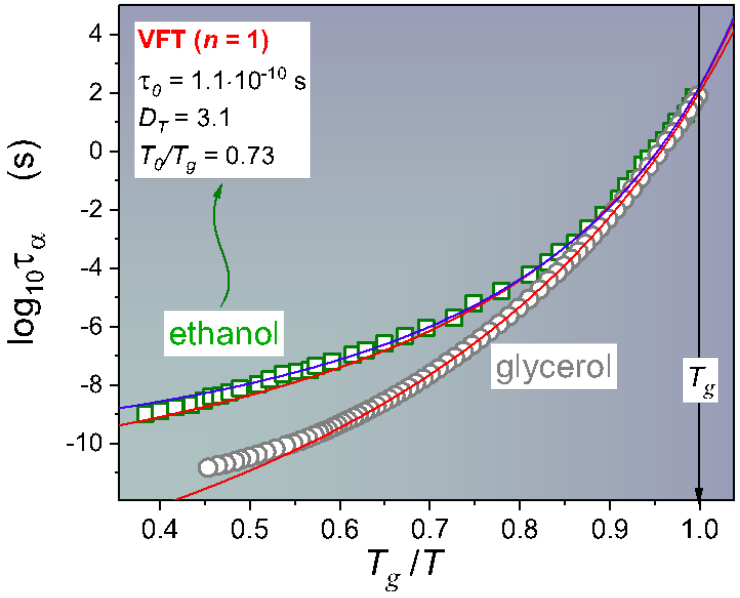
VFT (n = 1)
τ0 = 1.1·10-10 s
DT = 3.1
T0/Tg = 0.73
ethanol
glycerol
Tg
log10τα (s)
Tg / T

Fig. 4

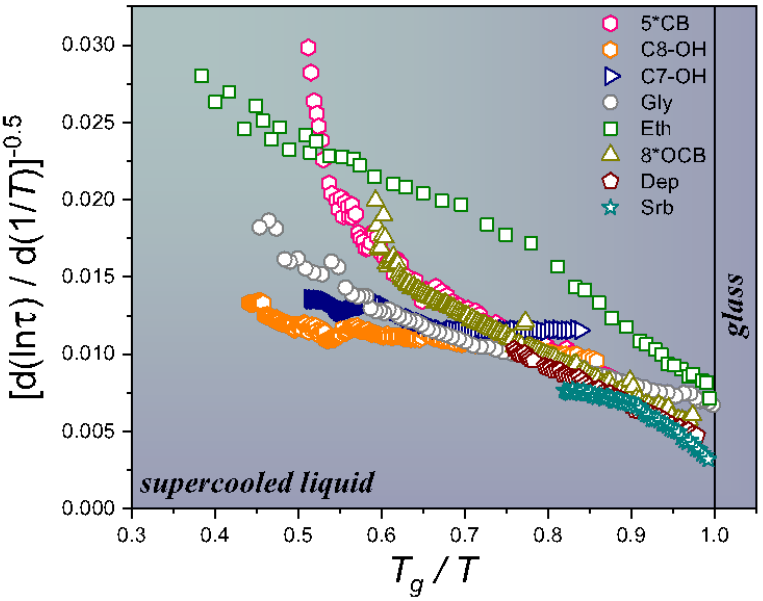
5*CB
C8-OH
C7-OH
Gly
Eth
8*OCB
Dep
Srb
supercooled liquid
glass
[d(lnτ) / d(1/T)]-0.5
Tg / T

Fig. 5

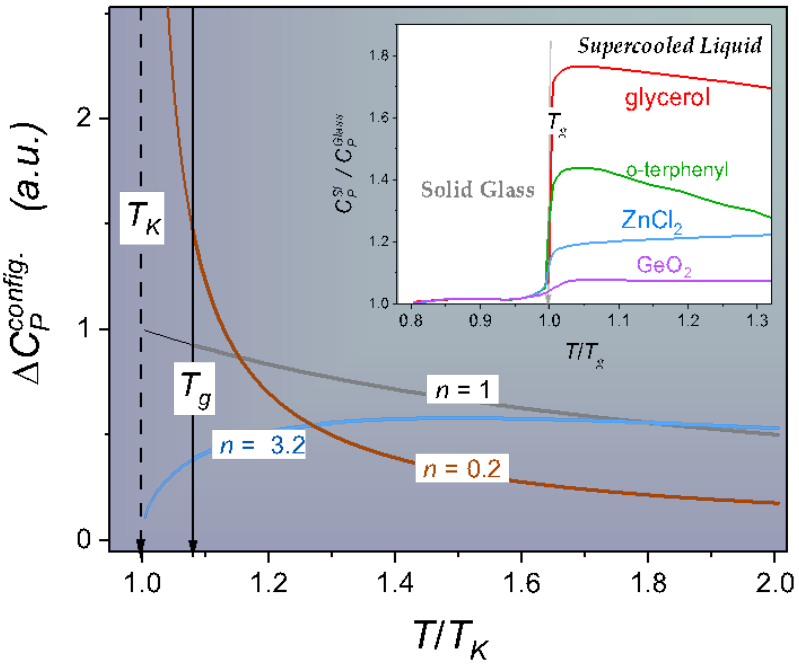
$\Delta C_P^{config.}$ (a.u.)
T/T_K
T_K
T_g
n = 1
n = 3.2
n = 0.2
Supercooled Liquid
glycerol
o-terphenyl
$ZnCl_2$
GeO_2
Solid Glass
C_P^{SL} / C_P^{Glass}
T/T_g

Fig. 6

Fig. 1 Tendency of usage of VFT and MYEGA relations. The number of research reports related to the VFT relation for supercooled glass-forming systems in the last two decades and papers associated with MYEGA one Eq. (11). Nowadays, the latter is a main competitor of the VFT relation. The figure was prepared by the use of Google Scholar.

Fig. 2 Configurational entropy for supercooled liquids. (A) Data portraying entropy behaviour for ethanol, glycerol, cyclooctanol and 5*CB liquid crystal. Red and blue straight lines denote Eq. (5) and Eq. (10) respectively. Dashed arrows present glass transition temperatures T_g. The insert shows configurational entropy as a function of reciprocal temperature $S_c(1/T)$ for all studied systems. **(B)** Configurational entropy normalised to the Kauzman temperature T_K for all samples basing on generalised Eq. (10). Impact of different n parameter on Eq. (10) is shown as an insert. Limit values $n = 0.1$ and $n = 2$ as well as classical case for $n = 1$ are marked by bold lines. Fitting parameters may be found in Table I.

Fig. 3 Distortions-sensitive analysis for the configurational entropy. Linearization $S_C(1/\mathrm{T}) = \mathrm{A} + Bx$, where $A = 1/nT_K, B = 1/n$ Eq. (15). All calculated parameters n corresponds well with ones obtained using Eq. (10) (see Table I).

Fig. 4 Evolutions of primary relaxation time for ethanol and glycerol presented in Angell plot. For glycerol $T_g = 187.7K$ and ethanol $T_g = 98.1K$. The inset shows results of the linearised, derivative-based analysis based on Eq. (7) and focused on revealing domains of the validity of the VFT portrayal (Eq. (2)): it is manifested via linear domains. The portrayal for ethanol in the inset, via the second-order polynomial, has the 'guide for eyes' meaning. Molecular structures of tested compounds are schematically shown. Experimental data in the central part of the plot are portrayed via the VFT Eq. (2) (in red) and the generalised VFT Eq. (13) (in blue), basing on the fitting domain $0.16 < T_g/T < 1$.

Fig. 5 Linearised distortions-distortions sensitive analysis ('Stickel plot'). Data are taken from the central parts of obtained results. Straight lines denote $n = 1$ and VFT description correctness. The temperature scale is normalised to T_g.

Fig. 6 Previtreous temperature dependencies of configurational component of heat capacity in supercooled glass-forming liquids. The values resulted from Eq, (4), present different parameters n. Thin curves are for the extrapolation into the solid glass state. The inset shows examples of patterns of heat capacity changes for a selected cooling rate: prepared based on Refs. 68, 69.